Acta Crystallographica Section F
Structural Biology and Crystallization Communications
ISSN 1744-3091

Structure of D-3-hydroxybutyrate dehydrogenase prepared in the presence of the substrate D-3-hydroxybutyrate and NAD$^+$

Md Mominul Hoque,[a,b] Satoru Shimizu,[a] Ella Czarina Magat Juan,[c] Yoshiteru Sato,[d] Md Tofazzal Hossain,[a,b] Tamotsu Yamamoto,[e] Shigeyuki Imamura,[e] Kaoru Suzuki,[f] Hitoshi Amano,[g] Takeshi Sekiguchi,[f] Masaru Tsunoda[h] and Akio Takénaka[a,h]*

[a]Graduate School of Bioscience and Biotechnology, Tokyo Institute of Technology, 4259 Nagatsuta-cho, Midori-ku, Yokohama, Kanagawa 226-8501, Japan, [b]Department of Biochemistry and Molecular Biology, University of Rajshahi, Rajshahi 6205, Bangladesh, [c]Graduate School of Science, The University of Tokyo, 7-3-1 Hongo, Bunkyo-ku, Tokyo 113-0033, Japan, [d]IGBMC, 1 Rue Laurent Fries, BP 10142, 67404 Illkirch, France, [e]Asahi Kasei Pharma Corporation, Tagat-gun, Shizuoka 410-2323, Japan, [f]College of Science and Engineering, Iwaki Meisei University, Chuodai-iino, Iwaki 970-8551, Japan, [g]Fukushima National College of Technology, Taira-kamiarakawa, Iwaki 970-8034, Japan, and [h]Faculty of Pharmacy, Iwaki Meisei University, Chuodai-iino, Iwaki 970-8551, Japan

Correspondence e-mail: atakenak@iwakimu.ac.jp

Received 4 February 2009
Accepted 9 March 2009

PDB Reference: D-3-hydroxybutyrate dehydrogenase, 3eew, r3eewsf.

D-3-Hydroxybutyrate dehydrogenase from *Alcaligenes faecalis* catalyzes the reversible conversion between D-3-hydroxybutyrate and acetoacetate. The enzyme was crystallized in the presence of the substrate D-3-hydroxybutyrate and the cofactor NAD$^+$ at the optimum pH for the catalytic reaction. The structure, which was solved by X-ray crystallography, is isomorphous to that of the complex with the substrate analogue acetate. The product as well as the substrate molecule are accommodated well in the catalytic site. Their binding geometries suggest that the reversible reactions occur by shuttle movements of a hydrogen negative ion from the C3 atom of the substrate to the C4 atom of NAD$^+$ and from the C4 atom of NADH to the C3 atom of the product. The reaction might be further coupled to the withdrawal of a proton from the hydroxyl group of the substrate by the ionized Tyr155 residue. These structural features strongly support the previously proposed reaction mechanism of D-3-hydroxybutyrate dehydrogenase, which was based on the acetate-bound complex structure.

1. Introduction

D-3-Hydroxybutyrate dehydrogenase (hereafter referred to as HBDH; EC 1.1.1.30) is found in a large variety of species ranging from unicellular microorganisms to higher primates. This ubiquitous enzyme catalyzes the reversible reaction between D-3-hydroxybutyrate and acetoacetate coupled to NAD$^+$/NADH conversion. Acetone is formed from the spontaneous decarboxylation of acetoacetate. D-3-Hydroxybutyrate, acetoacetate and acetone are collectively referred to as ketone bodies, although D-3-hydroxybutyrate is technically not a ketone but an alcohol. Ketone bodies are water-soluble compounds that are used as energy sources for the brain, kidney and heart (Laffel, 1999; Francois *et al.*, 1981). Ketone bodies are synthesized in the liver from acetyl-CoA when carbohydrate metabolism is impaired (Stryer, 1988). During starvation and vigorous exercise, D-3-hydroxybutyrate and acetoacetate can be converted back into two molecules of acetyl-CoA, which enters the TCA cycle as the main energy source. Although ketone bodies are valuable as energy sources, excess amounts lead to ketoacidosis. Diabetes is a major physiological cause of elevated blood ketones. HBDH is widely used in patients with diabetes mellitus to detect the presence of ketone bodies, which may be associated with diabetic ketoacidosis. The medical importance of this enzyme prompted us to determine its structure and to elucidate the details of its catalytic mechanism.

Several X-ray structures of HBDHs from various sources have recently been reported (Hoque *et al.*, 2008; Paithankar *et al.*, 2007; Ito *et al.*, 2006; Guo *et al.*, 2006). Based on the two crystal structures of HBDH from *Alcaligenes faecalis* (*Af*-HBDH), one in the apo form and another in a ternary complex with NAD$^+$ and acetate, we proposed a plausible reaction mechanism for the enzyme and the domain movement on NAD$^+$ and/or substrate binding and reviewed its structural development as a member of the short-chain dehydrogenase/reductase (SDR) family (Hoque *et al.*, 2008). In order to establish our previous proposals, we crystallized another ternary complex of *Af*-HBDH in the presence of the substrate D-3-hydroxy-

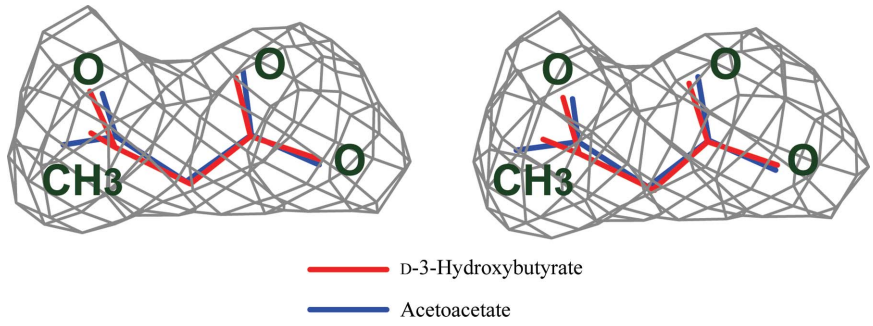

Figure 1
A stereoview of an $|F_o| - |F_c|$ OMIT map of the bound substrate D-3-hydroxybutyrate/product acetoacetate. The electron densities were contoured at the 3σ level with the program *O* (Jones *et al.*, 1991).

butyrate and NAD^+ and determined its crystal structure by X-ray analysis.

2. Materials and methods

2.1. Preparation and crystallization

Af-HBDH was expressed and purified using the methods described by Hoque *et al.* (2008). A lyophilized *Af*-HBDH sample was dissolved in 100 m*M* Tris–HCl buffer pH 8.5 to a concentration of 20 mg ml^{-1}. Crystallization conditions were surveyed at 277 and 293 K using the hanging-drop vapour-diffusion method. Crystals of the enzyme in complex with NAD^+ and the substrate D-3-hydroxybutyrate were obtained when 2 µl of the enzyme solution containing 5 m*M* NAD^+ were mixed with an equal volume of mother liquor consisting of 30%(*w*/*v*) PEG 4000, 0.2 *M* (*R*)-3-(−)-hydroxybutyric acid sodium salt and 100 m*M* Tris–HCl buffer pH 8.5 and equilibrated against 700 µl of the same mother liquor. Crystals of approximately 400 × 100 × 80 µm in size were obtained within 3 or 4 d at 293 K.

Table 1
Statistics of data collection and structure refinement.

Values in parentheses are for the highest resolution shell (3.1–3.0 Å).

Data collection	
X-ray source	PF BL6A
Wavelength (Å)	0.978
Resolution (Å)	50–3.0
Observed reflections	108159
Unique reflections	20947
Completeness (%)	91.6 (96.4)
R_{merge}† (%)	10.6 (32.1)
$I/\sigma(I)$	26.9 (9.5)
Space group	$P4_12_12$
Unit-cell parameters	
$a = b$ (Å)	91.1
c (Å)	261.0
Z‡	4
V_M ($Å^3$ Da^{-1})	2.5
Structure refinement	
Resolution (Å)	50–3.0
Reflections used	20937
R factor§ (%)	18.0
R_{free}¶(%)	23.5
No. of protein atoms	7624
No. of substrate atoms	28
No. of cofactor atoms	176
No. of ions	2 Ca^{2+}, 3 Cl^-
No. of water molecules	244
R.m.s. deviations	
Bond lengths (Å)	0.007
Bond angles (°)	1.3
Between subunits (Å)	0.35
Ramachandran plot (%)	
Most favoured regions	83.8
Additional allowed regions	15.3

† $R_{merge} = 100 \times \sum_{hkl}\sum_i |I_i(hkl) - \langle I(hkl)\rangle| / \sum_{hkl}\sum_i I_i(hkl)$, where $I_i(hkl)$ is the ith measurement of the intensity of reflection hkl and $\langle I(hkl)\rangle$ is its mean value. ‡ Number of subunits in the asymmetric unit. § R factor $= 100 \times \sum_{hkl} ||F_o| - |F_c|| / \sum_{hkl} |F_o|$, where $|F_o|$ and $|F_c|$ are the observed and calculated structure-factor amplitudes, respectively. ¶ Calculated using a random set containing 10% of the observations that were not included throughout refinement (Brünger, 1992).

2.2. X-ray data collection and processing

For data collection, suitable crystals were cryoprotected in mother liquor containing 30% glycerol and flash-frozen in liquid nitrogen for 30 s. X-ray experiments were performed at 100 K with synchrotron radiation on beamline BL6A (λ = 0.978 Å) of the Photon Factory (PF; Tsukuba, Japan). The diffraction patterns were recorded on an ADSC Quantum 4R detector positioned 174.6 mm away from the crystal; each frame was taken with a 10 s exposure time and with a 1° oscillation step over a range of 180°. Bragg spots were indexed and their intensities were estimated by integrating around them. Although the crystal diffracted to 2.3 Å resolution, it was difficult to integrate beyond 3.0 Å resolution because the spots were highly deformed in the outer region owing to damage on flash-freezing. Intensity data were then merged and scaled between the frames with the program *HKL*-2000 (Otwinowski & Minor, 1997). These data

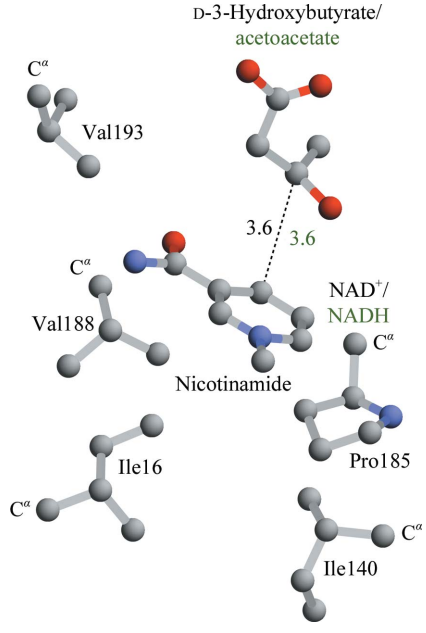

Figure 2
The hydrophobic residues surrounding the nicotinamide moiety in *Af*-HBDH. The product acetoacetate molecule and NADH are omitted for clarity.

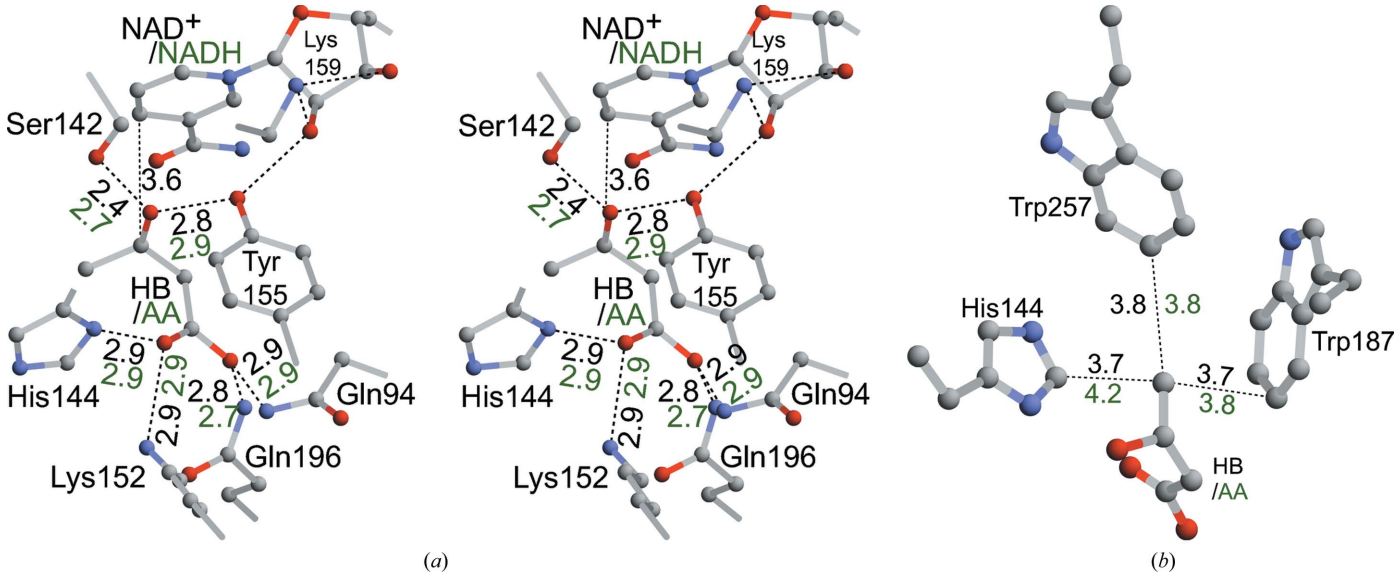

Figure 3
The D-3-hydroxybutyrate (HB) binding geometry in a subunit of the tetrameric *Af*-HBDH. (*a*) A whole view in stereo and (*b*) the three residues surrounding the methyl group of the substrate. Numbers indicate the atomic distances (in Å). The product acetoacetate molecule (AA) is omitted for clarity.

were further converted to structure-factor amplitudes with *TRUNCATE* from the *CCP*4 suite (Collaborative Computational Project, Number 4, 1994). The crystal data and the statistics of data collection are summarized in Table 1.

2.3. Structure determination and refinement

As the asymmetric unit contains four subunits, the initial crystal structure was derived by the molecular-replacement method with the program *AMoRe* (Navaza, 1994), using the tetrameric structure of native *Af*-HBDH (PDB code 2yz7; Hoque *et al.*, 2008) as a search model. The significance of the solution was confirmed on an electron-density map displayed by *QUANTA* (Accelrys Inc.). After rigid-body refinement, the atomic parameters were refined by the restrained maximum-likelihood least-squares technique in *REFMAC*5 from *CCP*4 (Murshudov *et al.*, 1997). The resulting structure was revised by interpreting OMIT maps at every residue. Water molecules were found in the $|F_o| - |F_c|$ map, large peaks in which were assigned as calcium and chloride ions based on their surroundings. The crystal used was obtained under the optimal reaction conditions with sufficient cultivation time. It was plausible to consider that almost all substrate molecules had been converted to the product molecules and some of them were retained as the substrate. However, distinction between the two molecules was difficult in an $|F_o| - |F_c|$ map at the present resolution because the shapes of the corresponding densities in the four subunits were able to accept both molecules owing to their similar shape, as shown in Fig. 1. A relatively large difference was seen at the positions of the methyl groups of the two molecules because the three O atoms of both molecules are fixed by the formation of hydrogen bonds to the protein amino-acid residues. As the electron densities corresponding to the methyl groups were commonly poor in the four subunits, it was assumed in further structural refinements that the two molecules were mixed. In such a case, the cofactors should also be coupled with the two molecules, respectively. In the subsequent refinements, the two states of the product coupled with NADH and of the substrate coupled with NAD^+ were included by assuming equal occupancy. The final refinements were performed with the program *CNS* (Brünger *et al.*, 1998). Statistics of the structure refinements are given in Table 1. All 260 residues of each subunit fitted well into the electron density. A Ramachandran plot (Ramachandran *et al.*, 1963) calculated using *PROCHECK* shows that 83.8% and 15.3% of the nonglycine residues fall into the most favoured and allowed regions, respectively. Figures showing the structural details were drawn with *PyMOL* (DeLano Scientific; http://www.pymol.org) and *RASMOL* (Sayle & Milner-White, 1995). Structural comparisons between subunits were carried out using *Swiss-PdbViewer* v.3.7 (http://www.expasy.org/spdbv/).

3. Results and discussion

3.1. Cofactor binding

The four subunits of the tetramer assembled by noncrystallographic 222 symmetry superimposed well on each other, with root-mean-square deviations of 0.3–0.4 Å for all C^α atoms. The cofactor NAD^+/NADH molecules in each subunit are bound in the same manner as described in the previous report of the enzyme complexed with NAD^+ and acetate (Hoque *et al.*, 2008) and the nicotinamide

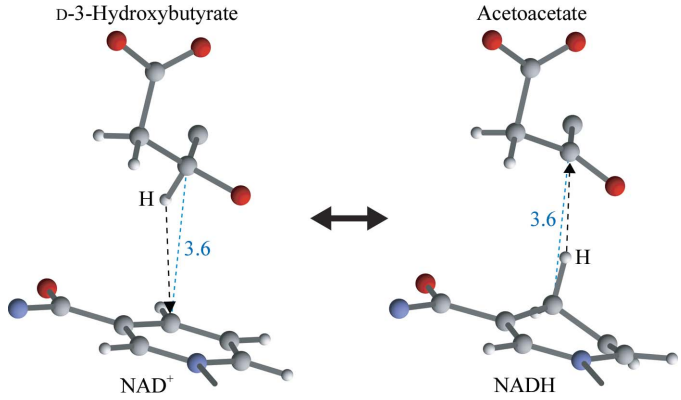

Figure 4
Structural images of the two states D-3-hydroxybutyrate:NAD^+ and acetoacetate:NADH.

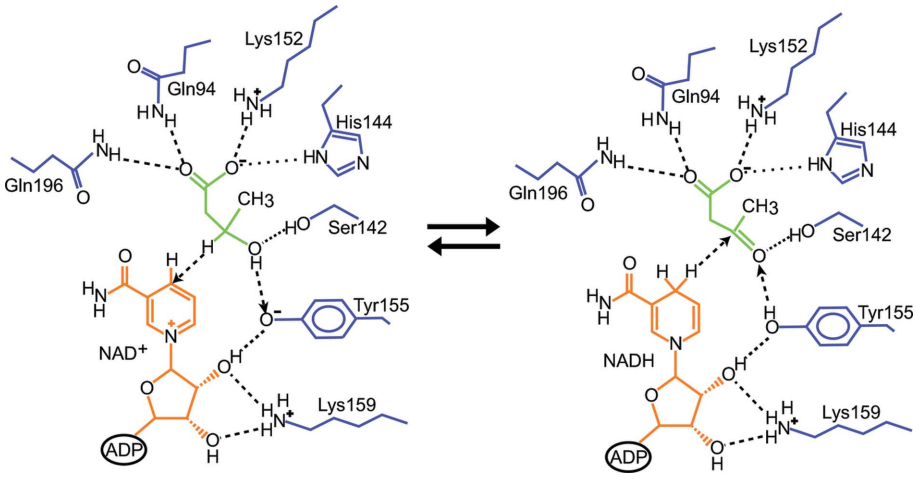

Figure 5
A schematic diagram of the *Af*-HBDH reversible reaction. The upper four residues form a substrate-specific variable region and the lower three residues are the catalytic amino acids conserved in the SDR family.

moiety is anchored in the hydrophobic cavity surrounded by Ile16, Ile140, Pro185, Val188 and Val193, as shown in Fig. 2.

3.2. Substrate binding

All the distances described in this section are values averaged over the four subunits. The binding geometries of the four substrates are quite similar to that of the model derived from the acetate-bound complex (Hoque *et al.*, 2008). The carboxylate groups of the substrate/product interact with the residues which bind the acetate carboxylate group, although their positions and orientations vary slightly owing to the size of the molecule. One of the two carboxylate O atoms is bound to Gln94 and Gln196 through two hydrogen bonds at distances of 2.8 (2.9)[1] and 2.8 (2.7) Å, respectively (Fig. 3). The other O atom forms two hydrogen bonds to His144 and Lys152 at distances of 2.9 (2.9) and 2.9 (2.9) Å, respectively. As suggested in the previous paper, the site at which a water molecule is trapped by Ser142 and Tyr155 in the acetate-bound complex is occupied by the hydroxyl O atom of the substrate or by the ketone O atom of the product, forming hydrogen bonds to these catalytic residues with distances of 2.4 (2.7) and 2.8 (2.9) Å, respectively. The methyl group of the substrate/product is accommodated in a small space that is surrounded by hydrophobic parts of His144, Trp187 and Trp257 at distances of 3.7 (4.2), 3.7 (3.8) and 3.8 (3.8) Å, respectively. The C3 atom of the substrate/product is positioned at a distance of 3.6 (3.6) Å away from the C4 atom of the nicotinamide ring of NAD^+/NADH.

3.3. Catalytic reaction mechanism

The crystal was obtained under the optimal reaction conditions at pH 8.5 (Asahi Kasei Enzymes T-68, 110-112, Asahi Kasei). It is reasonable to consider that substrate D-3-hydroxybutyrate molecules were converted to product acetoacetate molecules in the crystallization solution or in the crystalline state. Since the reaction is reversible, some of them are retained as the substrate or return from the product to the substrate in the equilibrium state. However, it is difficult to estimate their contents. The geometrical shapes of the two molecules are similar to each other apart from the configuration of the C3 atom (sp^3 or sp^2). Although at the present resolution it is difficult to distinguish which molecule is bound to the active site, the structure allowed us to suggest the following speculative reaction mechanism. D-3-Hydroxybutyrate must be coupled with NAD^+, while acetoacetate must be coupled with NADH, as shown in Fig. 4. In the forward reaction, the C3 atom of the substrate directs its H atom to the C4 atom of NAD^+. In the reverse reaction, the saturated C4 atom of NADH directs one of its two H atoms to the C3 atom of the product. Therefore, the conversion could proceed reversibly with a simple shuttle movement of a hydrogen negative ion between C3 and C4. Here, it is interesting to note that the product can only go back to the D form of 3-hydroxybutylate in the reverse reaction.

As shown in Fig. 5, the Tyr155 residue could be deprotonated at the optimal pH to withdraw a proton from the bound hydroxyl group of the substrate. This process facilitates carbonyl-bond formation in the substrate. At the same time, the hydrogen negative ion attached to the C3 atom of D-3-hydroxybutyrate is transferred to the C4 atom of the nicotinamide ring of NAD^+, thus producing acetoacetate and NADH. These events can be reversed for acetoacetate to be converted back to D-3-hydroxybutyrate. As pointed out in the previous paper (Hoque *et al.*, 2008), the Lys159 residue possibly plays two roles: assisting in the proper orientation of the coenzyme by forming hydrogen bonds to the hydroxyl O atoms of the nicotinamide-ribose moiety and lowering the pK_a value of Tyr155 by an electrostatic effect.

This work was supported in part by Grants-in-Aid for the Protein3000 Research Program from the Ministry of Education, Culture, Sports, Science and Technology of Japan. We thank S. Kuramitsu for organizing the research group in the program and N. Igarashi and S. Wakatsuki for facilities and help during data collection.

References

Brünger, A. T. (1992). *Nature (London)*, **355**, 472–475.
Brünger, A. T., Adams, P. D., Clore, G. M., DeLano, W. L., Gros, P., Grosse-Kunstleve, R. W., Jiang, J.-S., Kuszewski, J., Nilges, M., Pannu, N. S., Read, R. J., Rice, L. M., Simonson, T. & Warren, G. L. (1998). *Acta Cryst.* D**54**, 905–921.
Collaborative Computational Project, Number 4 (1994). *Acta Cryst.* D**50**, 760–763.
Francois, B., Bachmann, C. & Schutgens, R. (1981). *J. Inherit. Metab. Dis.* **4**, 163–164.
Guo, K., Lukacik, P., Papagrigoriou, E., Meier, M., Lee, W. H., Adamski, J. & Oppermann, U. (2006). *J. Biol. Chem.* **281**, 10291–10297.

[1] Values in parentheses are for the product acetoacetate.

Hoque, M. M., Shimizu, S., Hossain, M. T., Yamamoto, T., Imamura, S., Suzuki, K., Tsunoda, M., Amano, H., Sekiguchi, T. & Takénaka, A. (2008). *Acta Cryst.* D**64**, 496–505.
Ito, K., Nakajima, Y., Ichihara, E., Ogawa, K., Katayama, N., Nakahima, K. & Yoshimoto, T. (2006). *J. Mol. Biol.* **355**, 722–733.
Jones, T. A., Zou, J.-Y., Cowan, S. W. & Kjeldgaard, M. (1991). *Acta Cryst.* A**47**, 110–119.
Laffel, L. (1999). *Diabetes Metab. Res. Rev.* **15**, 412–426.
Murshudov, G. N., Vagin, A. A. & Dodson, E. J. (1997). *Acta Cryst.* D**53**, 240–255.
Navaza, J. (1994). *Acta Cryst.* A**50**, 157–163.
Otwinowski, Z. & Minor, W. (1997). *Methods Enzymol.* **276**, 307–326.
Paithankar, K. S., Feller, C., Kuettner, E. B., Keim, A., Grunow, M. & Sträter, N. (2007). *FEBS J.* **274**, 5767–5779.
Ramachandran, G. N., Ramakrishnan, C. & Sasisekharan, V. (1963). *J. Mol. Biol.* **7**, 95–99.
Sayle, R. & Milner-White, E. J. (1995). *Trends Biochem. Sci.* **20**, 374–376.
Stryer, L. (1988). *Biochemistry*, 3rd ed., pp. 478–480. New York: W. H. Freeman & Co.